Investigating the Low-State of NGC 1275 with VERITAS and Multi-Wavelength Observations

Anjana Kaushik Talluri[1]; for the VERITAS Collaboration[2]

[1]University of Minnesota

[2]https://veritas.sao.arizona.edu

Credit: Center for Astrophysics | Harvard & Smithsonian

Motivations

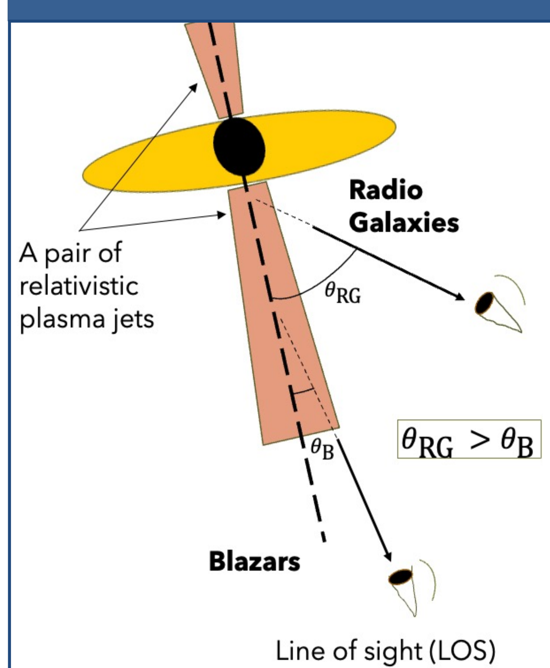

Figure 1. Pictorial depiction of the jet-viewing angles of blazars and radio galaxies with respect to the line of sight; the latter tend to have larger jet-viewing angles to LOS as indicated in the image.

- At Very-High-Energies (VHE; E>100 GeV), the dominant extragalactic sources are blazars, with very few radio galaxies (RG) e.g., NGC 1275, Cen A, M87 and 3C 264. As with blazars, the physical origin of TeV emission in these RG remains unclear.
- Large jet-viewing angles in RG -> low Doppler factor -> detection bias to nearby RG.
- Characterizing the low-state behavior of a source is crucial to gain further insights into its flaring states & variability.
- Compared to their bright, flaring states, low-flux states of jetted active galactic nuclei require longer integration times for a detection.
- **Objective:** characterize both flaring and non-flaring states of NGC1275 to understand gamma-ray emission mechanisms.
- **Current study:** Low-state multi-wavelength SED over 2012-2017 fit to a single-zone Synchrotron self-Compton model.

NGC 1275 (3C 84)

- NGC 1275 (z=0.01756), central galaxy in the Perseus cluster, is host to an extremely bright compact radio source (3C 84). It has a complex morphology that has evolved with time.
- **Previous low-state studies:** Aleksić+2014 utilized MAGIC observations from 2009-2011 and attempted to explain the low-state emission with a single-zone SSC model.
- **Significant NGC 1275 flare in January 2017:** Multiwavelength (MWL) SED fitting of the 2017 flare data indicates that a multi-zone SSC model (with two SSC components) and a strong external inverse-Compton (EIC) component is required (Rulten+ in prep). The model points towards radio component C3 as the emission region of the flare.
- **Another significant NGC 1275 flare in December 2022:** Detected by MAGIC (Atel #15820; 150% Crab) and LST-1 (Atel #15819; ~140% Crab). Follow-up observations by VERITAS coordinated with *Swift*-XRT and *NuSTAR* on Dec 29th, 2022.

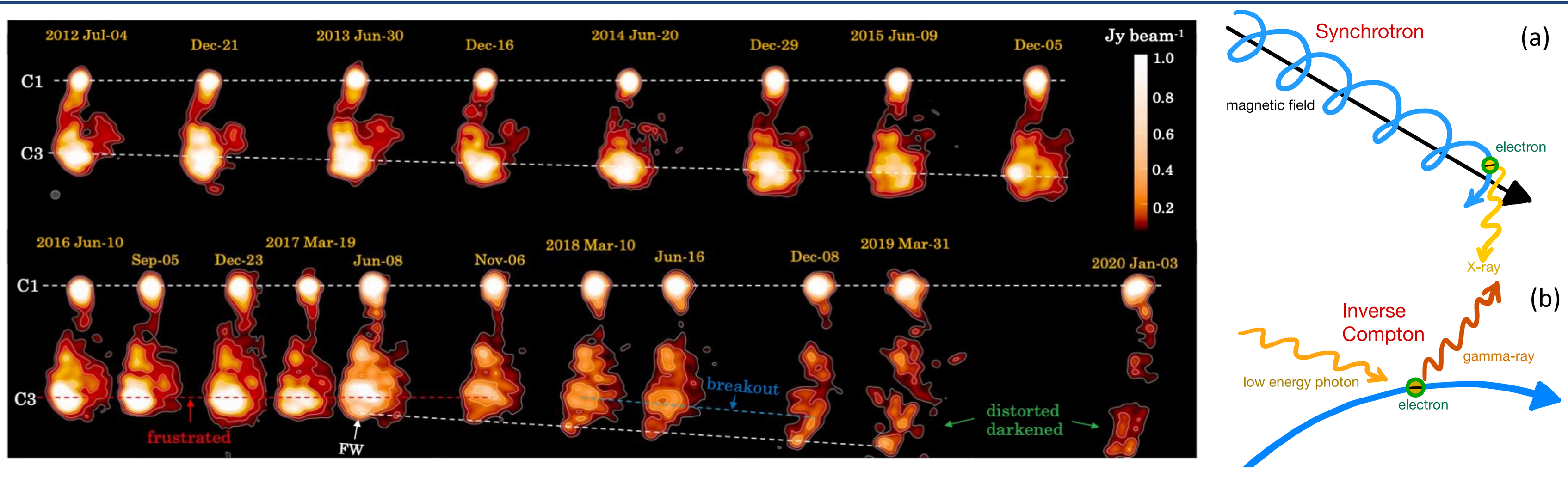

Figure 2. (Left) Sequence of images from VLBA observations of 3C 84 over 2012-2020 showing the changes in C3, an emission component, and evolution in the overall radio morphology (Credit: Kino+2021). **(Right)** Pictorial depictions of the Synchrotron emission process in **(a)** and inverse-Compton emission process in **(b)**.

Multi-wavelength Low-State Data Selection

Light curves were constructed for each waveband across 2012-2017.

↓

Two Stage Thresholding technique was applied.
Threshold* = μ + (3×σ)
First iteration: most significant flares.
Second iteration: any potential high states.

↓

If a flare was identified in one band, simultaneous data were removed from the other bands as well.

↓

All data were restricted to VERITAS observing windows of NGC 1275.

*For the Fermi-LAT data selection alone, the flare threshold utilized was different: data exceeding three median-absolute-deviations from the median (Talluri+2023).

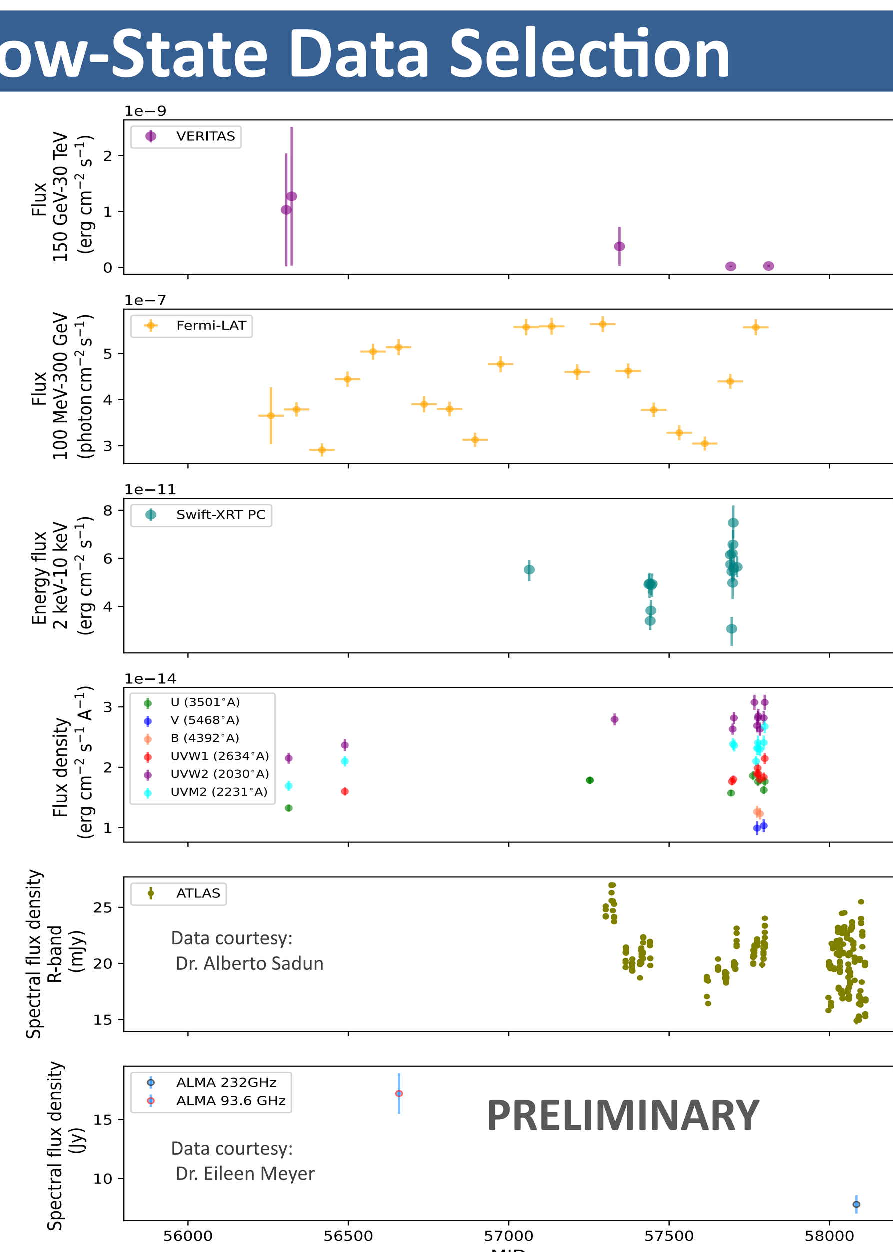

Figure 3. (Right) Panel of (preliminary) MWL light curves with flux on the y-axis and the observation date in MJD on the x-axis spanning 2012-2017. All the data shown here are contemporaneous with VERITAS observing windows of NGC 1275.

VERITAS Analysis

- VERITAS low state results are displayed in Table 1.
- The VERITAS low-state flux is comparable to MAGIC low-state flux reported in Aleksić+2014: 3% Crab (Camp I, Oct 2009-Feb 2010) and 2.4% Crab (Camp II, Oct 2010-Feb 2011).

Exposure (h)	Significance	VTS Flux (>200 GeV) ($cm^{-2}s^{-1}$)	γ	N ($TeV^{-1}m^{-2}s^{-1}$)	E_0 (TeV)
53	20σ	(4.8±0.3)E-12 ~2.2% Crab	3.86±0.2	(4.68±0.5)E-08	0.4

Table 1: Summary of VERITAS low-state analysis

Power-law: $$\frac{dN}{dE} = N\left(\frac{E}{E_0}\right)^{-\gamma} \quad (1)$$

Fitting of the Low-State Inverse-Compton SED Peak

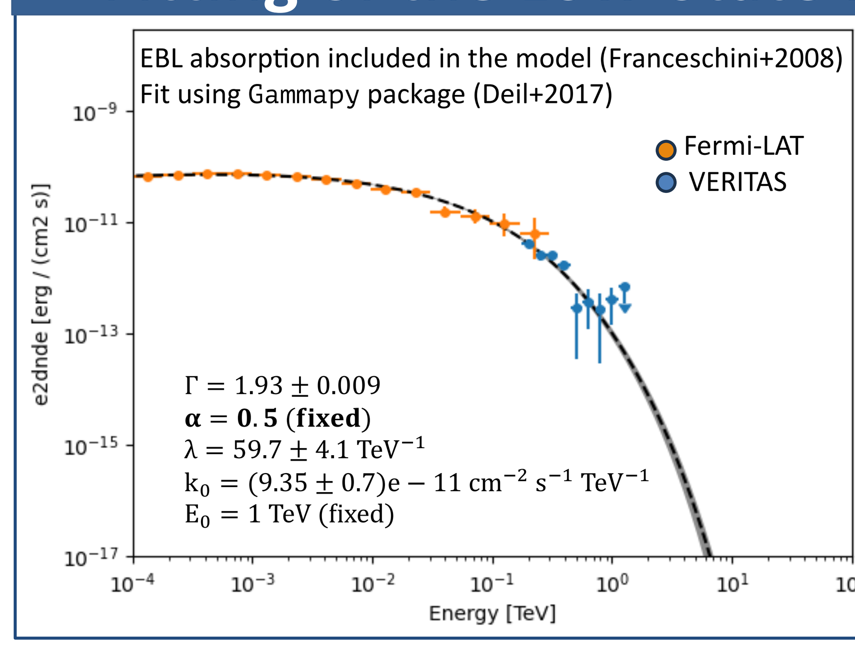

- Akaike Information Criterion test to determine best fitting model: Power-law + sub-exponential cutoff model (eqn 2) with a cutoff energy of 16 GeV (Talluri+2023).

$$\frac{dN}{dE} = k_0\left(\frac{E}{E_0}\right)^{-\Gamma}\exp(-(\lambda E)^{\alpha}),\ \alpha = 0.5 \quad (2)$$

Figure 4. (Left) Low-State Compton SED peak fit with the best fitting model: a power-law + sub-exponential cutoff (Talluri+23).

Fitting of the Low-State Multi-wavelength SED

- Multi-wavelength data was fit to a single-zone SSC with the latest version of `Bjet_MCMC` tool (Hervet+2023). The underlying leptonic particle distribution was assumed to be a broken power-law with the parameters shown in Table 2.
- The Doppler factor was constrained (δ< 3.2) to keep it consistent with Rulten+ in prep which adopted a jet viewing angle of 18°.
- Hyperparameters of the MCMC fit: nsteps =6500, nwalkers=200, and burnin=250.

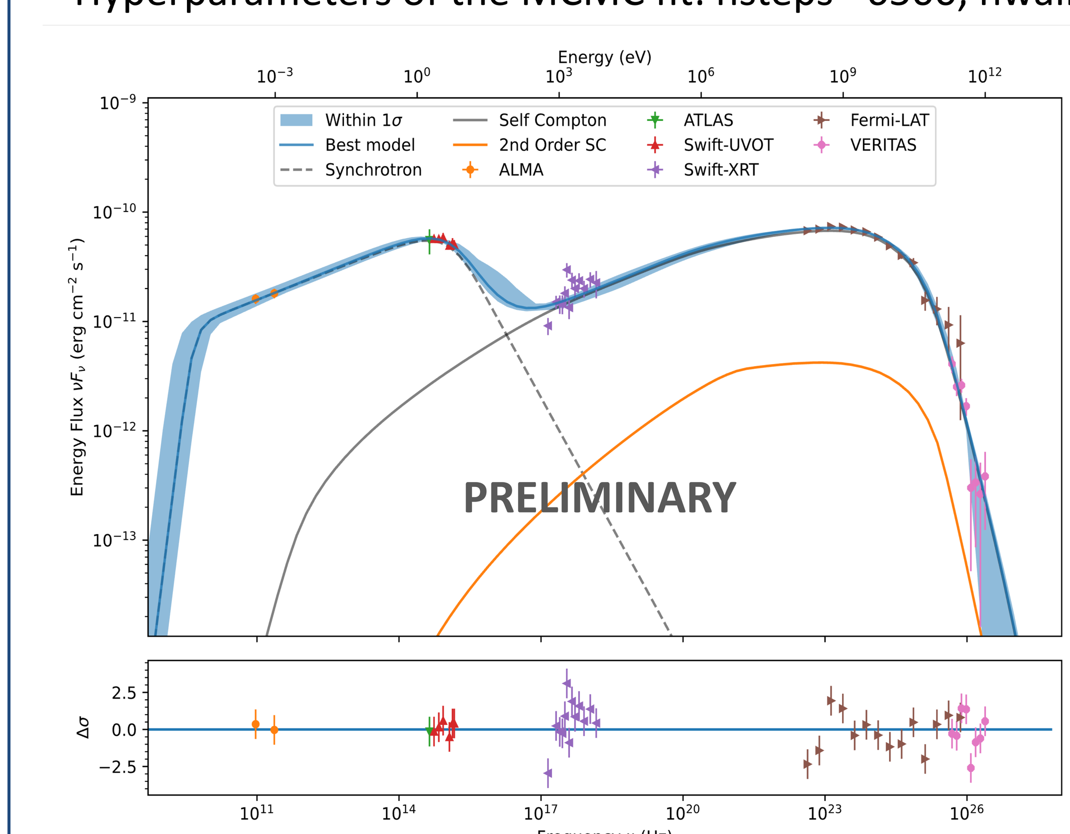

Figure 5. Low-state MWL SED with data from 2012-2017 fit to a single-zone SSC model. The best fit and the 1σ errors are shown in blue. The synchrotron peak is indicated by a dotted line and the inverse-Compton peak in a solid black line. The second order SSC component is shown in orange.

Parameter	Best value
Doppler factor ($\delta < 3.2$)	$2.48^{+0.22}_{-1.42}$
Particle density factor (K) [$10^3 cm^{-3}$]	$7.4^{+12.3}_{-6.3}$
First index (α_1)	$2.7^{+0.04}_{-0.05}$
Second index (α_2)	$4.6^{+0.4}_{-1.0}$
Low-energy cutoff	$6.5^{+28.5}_{-5.5}$
High energy cutoff [10^5]	576^{+424}_{-571}
Energy break [10^5]	$1.04^{+0.95}_{-0.38}$
Magnetic field strength (B) [10^{-3}G]	$7.59^{+8.81}_{-4.12}$
Blob radius R [10^{18}] [cm]	$2.3^{+7.7}_{-1.3}$
Reduced chi squared	66.93 / 35 = 1.83

Table 2. Best fitting model parameters along with their 1σ errors

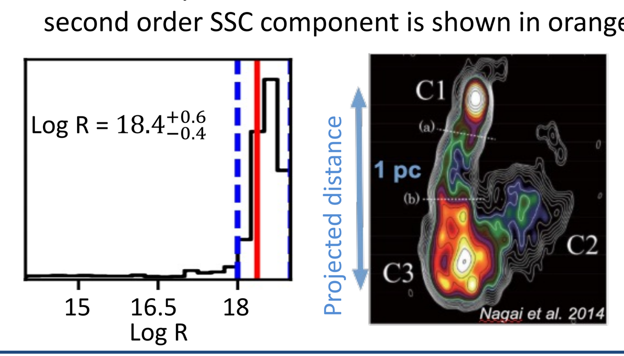

Figure 6. (Left) Posterior distribution of the radius of the emission region (R). The best fitting radius is 2×10^{18} cm or 0.76 pc (shown in red). The 1σ range on R is 0.3 pc to 3.2 pc (shown in blue). **(Right)** 43 GHz total intensity map of 3C 84 from Nagai+2014. The overall scale (projected distance) between C1 (radio core) and C3 (radio component) is indicated on the image. The de-projected distance of C3 from the core (assuming θ=18°) based on Nagai+14 is ~3.2 pc.

Conclusions & Future Work

- This is the first comprehensive exploration of single-zone SSC parameter space in the low state SED of NGC1275 with data extending from radio to VHE γ-rays.
- The model shows a convincing SED fit when considering an angle with the line of sight of 18°. A large emission zone is favored of at least 0.3 pc (1σ C.L.).
- Such a large emission region may not be accommodated by emission from the core, suggestive of the radio-zone C3 as a potential TeV emitter in the low state, consistent with the 2017 flare state model in Rulten+ in prep.
- An ongoing investigation of the 2022 flare including the MWL SED is currently in progress.

Contact

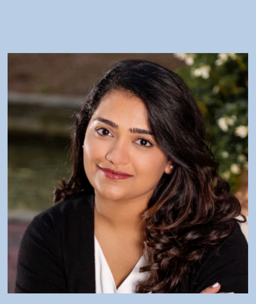

Anjana Kaushik Talluri
University of Minnesota
Email: telid001@umn.edu

References

1. Aleksić J., et al., 2014, A&A, 564, A5
2. Blanch O., Nievas Rosillo M., Arbet-Engels A., Nigro C., Molero M., 2022, ATel, 15820
3. Cortina & CTA LST Collaboration, 2022, ATel, 15819
4. C. Deil, R. Zanin, J. Lefaucheur, et al., 35th International Cosmic Ray Conference (ICRC2017), volume 301 of International Cosmic Ray Conference, 2017, p. 766
5. Franceschini A et al. 2008 A&A. 487:837
6. Hervet, O.,et al. 2023 arXiv:2307.08804
7. Kino, M., Niinuma, K., Kawakatu, N., et al. 2021, ApJL, 920, L24
8. Nagai, H., Haga, T., Giovannini, G., et al. 2014, ApJ, 785 53
9. Rulten et al., in prep
10. Talluri A. K., VERITAS Collaboration 2023, in 38th ICRC. p. 661
11. Tavecchio, F., & Ghisellini, G. 2014, Monthly Notices of the Royal Astronomical Society, 443, 1224

Acknowledgements

This research was partially supported by the National Science Foundation under grants PHY 2110737 and DGE-1922512. This research is supported by grants from the U.S. Department of Energy Office of Science, the U.S. National Science Foundation and the Smithsonian Institution, by NSERC in Canada, and by the Helmholtz Association in Germany. This research used resources provided by the Open Science Grid, which is supported by the National Science Foundation and the U.S. Department of Energy's Office of Science, and resources of the National Energy Research Scientific Computing Center (NERSC), a U.S. Department of Energy Office of Science User Facility operated under Contract No. DE-AC02-05CH11231. We acknowledge the excellent work of the technical support staff at the Fred Lawrence Whipple Observatory and at the collaborating institutions in the construction and operation of the instrument.